Journal of Engineering Research and Applied Science
Available at www.journaleras.com
Volume 14 (2), December 2025, pp 250-263
ISSN 2147-3471 © 2025

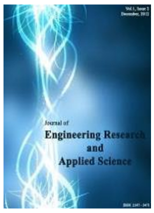

Geochemical Baseline Establishment for Exploration and Environmental Assessment: The Soil–Rock Relationship in the Gümüşhane Granitoid, Eastern Pontides, Türkiye

Alaaddin Vural*

Geological Engineering, Faculty of Engineering, Ankara University, Ankara, Türkiye
https://orcid.org/0000-0002-0446-828X

Accepted 16 December 2025

Abstract

Geochemical baseline data are essential for both mineral exploration and environmental assessment, particularly in regions where naturally elevated element concentrations may mask or mimic mineralization-related anomalies. This study establishes robust soil and rock geochemical baselines for the Early–Late Carboniferous Gümüşhane Granitoid, a key lithological unit situated within one of Türkiye's major metallogenic provinces in the Eastern Pontides. A total of 16 granitoid and 34 overlying soil samples were analyzed using ICP–MS, and the resulting dataset was evaluated through descriptive statistics, Pollution Index (PI), and Index of Geo-accumulation (*Igeo*) calculations.

The granitoid bedrock exhibits PI values close to 1.0 and Igeo values near −0.5 for major oxides, indicating compositions consistent with typical upper continental crust and reflecting unmodified litho-geochemical signatures. Trace-element patterns reveal notable depletions in Co, Cs, V, Ni, and Pb, whereas slight enrichments in Ba, Ga, Y, and rare earth elements likely reflect secondary mineral phases or mild hydrothermal modification. Soil samples, however, display markedly elevated PI values (>1.5) for a broad suite of elements including P, Mn, As, Y, Cd, Sn, Sb, REEs, Pb, Th, and U, demonstrating that soils developed on the granitoid host naturally enriched background levels far above global crustal averages.

Median, MAD, and Median + 2×MAD thresholds were used to identify conservative and high-level anomaly limits, offering a statistically robust framework suited for non-normally distributed soil datasets. These locally calibrated thresholds provide critical guidance for mineral exploration, as reliance solely on universal crustal reference values could lead to false anomaly detection. From an environmental perspective, the established background levels allow for a more accurate distinction between natural geochemical signatures and anthropogenic contributions.

Overall, this study provides the first integrated soil–rock geochemical baseline for the Gümüşhane Granitoid and delivers a scientifically rigorous reference framework for both exploration geochemistry and environmental monitoring across the Eastern Pontides.

Keywords: *Gümüşhane Granitoid, Soil geochemistry, Element enrichment, Geochemical prospecting, Local threshold values*

1. Introduction

Soil geochemistry studies are widely employed both in exploration geochemistry for mineral prospecting and in environmental geochemistry. The data generated from such studies often serve both purposes, and their interpretation may therefore converge. In particular, geochemical investigations that address environmentally relevant, naturally derived risks inherently focus on elements occurring at elevated concentrations, which can also provide a valuable basis for mineral exploration. One of the key factors influencing the elemental composition of soils is the parent rock from which the soils are derived. Considering this factor, the present study aims to evaluate soil–rock relationships by examining the concentrations of selected elements in soils and their corresponding parent rocks in the Gümüşhane region—one of Türkiye's major metallogenic belts.

The Gümüşhane region and its surroundings host several significant mineral deposits [1, 2, 11–18, 3–10]. This region is an important natural resource area within the Tethyan metallogenic belt and hosts a variety of magmatic–hydrothermal deposit types, including porphyry (Cu–Mo, Cu–Au, etc.), epithermal (Au, Au–Ag), and volcanic massive sulfide (Cu–Pb–

*Corresponding author: alaaddinvural@gmail.com

Zn) mineralizations. Therefore, numerous mineral exploration studies have been conducted in the region, and, owing to its elevated elemental background levels, various environmental geochemistry investigations have also been carried out [14, 19–25].

One of the most essential components of mineral exploration is geochemical prospecting (reconnaissance) studies. Numerous mineral deposits have been identified through such investigations [1, 26–31]. While the fundamental components of prospecting studies consist of stream-sediment, soil geochemistry, and plant geochemistry, more detailed exploration includes rock-geochemistry analyses.

One of the most critical factors determining the success of prospecting studies is the accurate identification of elemental baseline values and anomaly thresholds [12, 32–37].

This study aims to determine, through robust scientific methods, the geochemical background and threshold concentrations of selected major and trace elements in the Gümüşhane Granitoid—which forms extensive exposures within the Gümüşhane province—and in the soils derived from this lithological unit.

The resulting values will constitute a dependable reference framework for exploration geochemistry by assisting in the recognition of potential mineralization-related anomalies and supporting geochemical prospecting strategies in the area.

From the perspective of environmental geochemistry, the locally established background levels will provide an essential benchmark for distinguishing natural geochemical signatures from anthropogenic inputs. Consequently, these data will contribute to more accurate environmental risk evaluations and inform evidence-based land-management and planning efforts.

2. Material and Method

2.1. Regional Geology

The pre-Tertiary geological framework of the Eastern Pontides consists of a diverse assemblage of lithological units. These include metamorphic rocks of Early Carboniferous age [38], followed by extensive plutonic bodies emplaced during the Early to Late Carboniferous ([39–47]. Volcano-sedimentary successions formed in the Early to Middle Jurassic are also widely exposed [48, 49]. Middle–Late Jurassic magmatism is represented by several plutonic intrusions [47, 50–54]. This succession is overlain by Early Cretaceous (Berriasian–Aptian) carbonate platforms. The geological record is further complemented by Late Cretaceous volcanic, plutonic, and sedimentary units that mark sustained magmatic and sedimentary activity during this period [55–60].

The Tertiary units of the Eastern Pontides comprise a broad spectrum of magmatic and volcanic rocks. These include Late Paleocene–Early Eocene adakitic lithologies [61–64], followed by extensive Early–Middle Eocene volcanic to subvolcanic suites [65–73]. Middle Eocene magmatism is further represented by a series of plutonic intrusions [2, 5, 11, 64, 74–81]. The volcanic activity continued into the Late Eocene and Oligocene [82, 83], and a suite of Miocene–Pliocene adakitic to non-adakitic volcanic and subvolcanic rocks is also present in the region [84]. The youngest geological units in the area consist of Quaternary alluvium, slope debris, and travertine deposits [85, 86].

The study area is located to the south and southeast of Gümüşhane, covering the Çamlıköy and Işıkdere localities, where the Early–Late Carboniferous Gümüşhane Granitoid is extensively exposed (Figure 1). A well-developed soil profile, of suitable thickness for soil geochemical investigations, has formed upon this granitoid bedrock.

2.2. Analytical Procedures

The preparation of soil samples—and a subset of rock samples—was carried out in the sample preparation laboratory of the Department of Geological Engineering at Gümüşhane University. Most of the chemical analyses were performed at the Gümüşhane University Central Laboratory using inductively coupled plasma–mass spectrometry (ICP–MS). Before analysis, the samples were dried, homogenized, and powdered to analytical grain size following standard geochemical preparation protocols.

Both the sample preparation workflow and instrumental analytical methodology adopted in this study are consistent with previously established procedures documented in Vural et al. [87], Vural and Şahin [88], and Bulut et al. [89]. These references outline the digestion methods, calibration strategies, quality control measures, and instrument performance criteria applied in similar geochemical investigations. Accordingly, appropriate blanks, duplicates, and certified reference materials were incorporated into the analytical sequence to ensure accuracy and reproducibility of the obtained data.

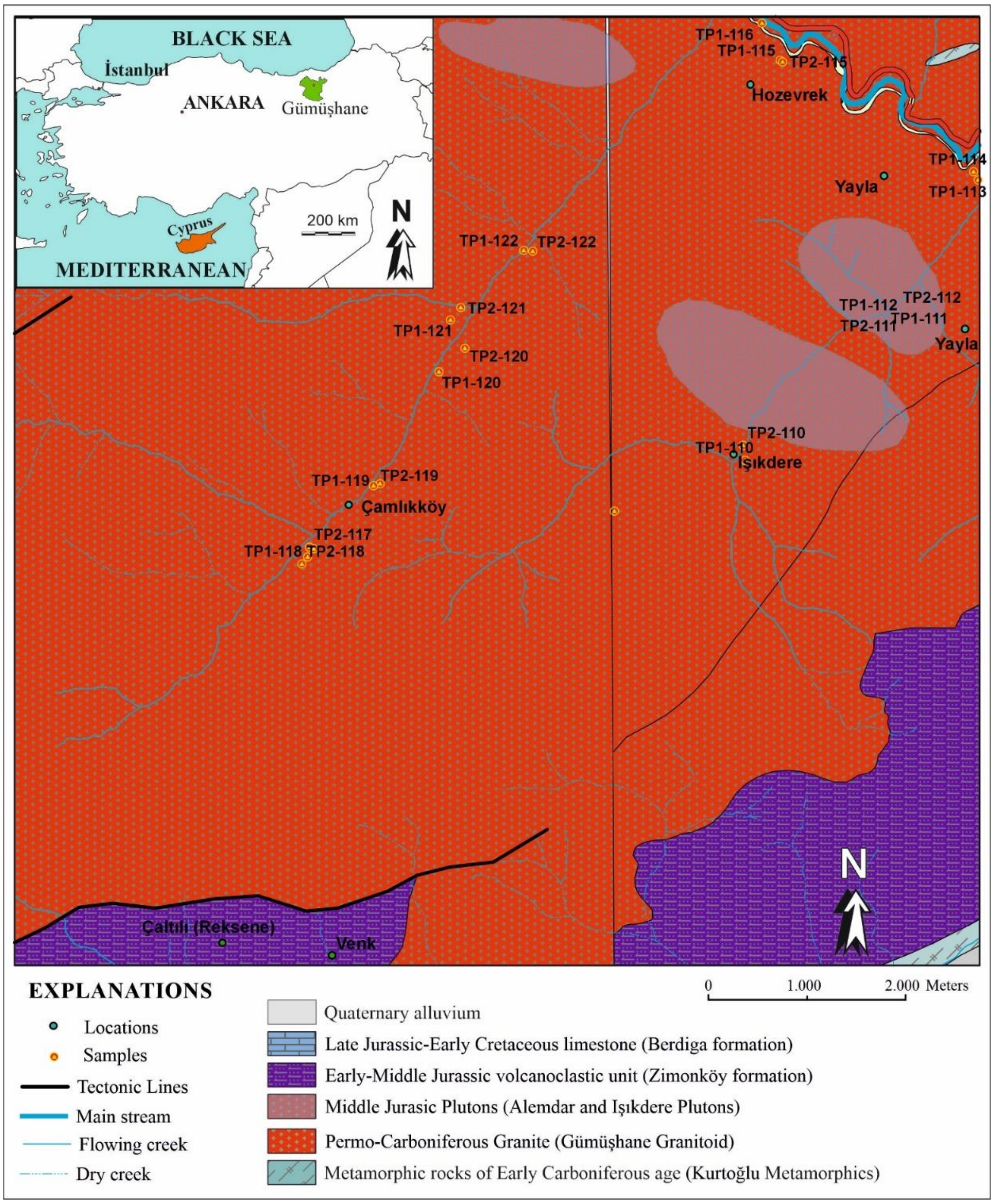

Figure 1. Geological map of the study area and sample locations [after 53, 54].

3. Results and Discussions

To establish reliable local elemental baseline values for the soils and bedrock of the Çamlıköy and Işıkdere districts (Gümüşhane province), a dataset comprising 16 granitoid rock samples and 34 soil samples was evaluated (Tables 1 and 2). The granitoid dataset integrates previously published geochemical analyses, including six samples from Lermi [20], nine samples from Dokuz [90], and seven samples published by Vural et al. [91]. These samples collectively represent the geochemical variability of the Early–Late Carboniferous Gümüşhane Granitoid, which dominates the bedrock geology of the study area.

Descriptive statistical parameters were calculated for both the soil and rock datasets. In addition to these measures, pollution/enrichment indices, namely the Pollution Index (PI) and the Index of Geo-accumulation (*Igeo*), were computed to assess the degree of elemental enrichment relative to upper continental crust (UCC) values. For this purpose, the

UCC concentrations of Rudnick and Gao [92] were adopted as reference compositions.

After calculating PI and Igeo values for each sample, descriptive statistics for these indices were also derived to characterize the enrichment tendencies of individual elements. Although the mean, median, and geometric mean values of the granitoid samples exhibit relatively close distributions (Figure 2), median values were preferred as representative central tendencies in order to reduce the influence of extreme values. Based on these median values, elemental threshold concentrations in the granitoid were determined using the widely applied robust estimators Median + MAD and Median + 2×MAD, where MAD corresponds to the median absolute deviation.

Table 1. Mean major oxide and trace-element concentrations of the Gümüşhane Granitoid exposed in the study area, together with calculated PI and Igeo indices. *Major oxides are reported in wt.%, whereas all trace elements are expressed in ppm*

	Mean	**Median**	**Geo.Mean.**	**PI**	**Igeo**
SiO_2	62.98	64.46	62.56	0.97	-0.63
Al_2O_3	16.65	16.45	16.58	1.07	-0.49
Fe_2O_3	5.38	4.84	4.57	0.96	-0.64
MgO	2.26	2.11	1.79	0.85	-0.82
CaO	4.10	3.89	3.29	1.08	-0.47
Na_2O	3.43	3.34	3.40	1.02	-0.56
K_2O	2.45	1.84	2.04	0.66	-1.18
TiO_2	0.80	0.67	0.67	1.05	-0.51
P_2O_5	0.21	0.16	0.17	1.07	-0.49
MnO	0.09	0.07	0.07	0.70	-1.10
Sc	6.33	7.00	6.07	0.49	-1.62
Ba	745.05	739.05	652.37	1.18	-0.35
Co	10.99	8.00	8.43	0.46	-1.70
Cs	1.96	1.80	1.76	0.37	-2.02
Ga	20.35	20.40	20.12	1.17	-0.36
Hf	6.14	5.30	5.52	1.00	-0.58
Nb	11.35	10.40	10.54	0.87	-0.79
Rb	80.33	78.05	65.60	0.93	-0.69
Sr	343.10	335.95	320.44	1.05	-0.51
Ta	0.84	0.80	0.80	0.89	-0.75
Th	11.56	8.15	8.91	0.78	-0.94
U	2.15	1.60	1.74	0.59	-1.35
V	6.00	6.00	6.00	0.06	-4.64
W	1.47	0.90	0.99	0.47	-1.67
Zr	229.98	190.50	197.86	0.99	-0.60
Y	27.93	25.10	26.38	1.20	-0.32
La	41.07	32.20	34.69	1.04	-0.53
Ce	88.57	70.50	76.41	1.12	-0.42
Pr	9.09	7.85	8.35	1.11	-0.43
Nd	29.97	26.60	28.76	0.99	-0.60
Sm	6.66	6.35	6.35	1.35	-0.15
Eu	1.41	1.31	1.31	1.31	-0.20
Gd	5.65	5.34	5.32	1.34	-0.16
Tb	0.89	0.83	0.84	1.19	-0.33
Dy	5.08	4.85	4.79	1.24	-0.27
Ho	0.95	0.89	0.89	1.07	-0.49
Er	2.82	2.65	2.66	1.15	-0.38
Tm	0.42	0.39	0.39	1.30	-0.21
Yb	2.65	2.66	2.47	1.33	-0.17
Lu	0.40	0.39	0.38	1.26	-0.25
Pb	6.12	6.70	5.73	0.39	-1.94
Ni	6.25	5.90	5.24	0.13	-3.49

Table 2. Descriptive statistics and MAD values of some element concentrations (ppm) in soils from the Çamlıköy and Işıkdere areas

	Mean	Median	S.Dev.	Max.	Min	MAD	M+MAD	M+2*MAD
Mg	1.14	1.14	0.42	2.25	0.19	0.22	1.36	1.58
P	986.90	837.59	474.01	2246.90	209.04	220.22	1057.81	1278.03
K	2.40	2.02	1.71	6.78	0.14	1.10	3.13	4.23
Ca	1.68	0.96	1.69	6.21	0.20	0.37	1.32	1.69
Sc	18.92	19.96	8.34	35.41	5.10	4.04	24.00	28.05
V	109.97	116.21	46.99	219.89	19.00	28.95	145.17	174.12
Cr	44.66	39.05	31.45	157.37	11.70	19.15	58.20	77.36
Mn	1463.76	1394.37	594.16	3772.90	732.00	235.49	1629.86	1865.35
Fe	5.81	5.57	2.16	9.75	2.60	1.71	7.27	8.98
Co	15.12	13.69	5.54	36.60	8.50	2.88	16.58	19.46
Ni	17.57	15.45	11.07	60.40	4.54	3.83	19.28	23.10
Cu	29.99	23.84	25.62	126.23	5.48	8.73	32.57	41.30
Zn	152.33	94.38	186.55	905.17	51.32	22.77	117.15	139.93
As	15.41	10.62	13.36	59.44	4.00	3.77	14.40	18.17
Se		0.64				0.37	1.01	1.10
Rb	121.63	123.90	85.47	360.78	7.00	56.32	80.22	236.55
Sr	94.97	78.80	81.57	475.01	10.00	21.04	99.84	120.87
Y	42.16	46.80	17.44	70.70	11.37	12.84	59.64	72.48
Mo	2.06	1.27	2.07	9.50	0.40	0.44	1.71	2.15
Cd	0.64	0.29	1.30	7.40	0.10	0.06	0.35	0.42
Sn	6.50	6.50	4.09	14.53	0.60	3.07	9.57	12.64
Sb	1.25	0.73	1.11	3.70	0.10	0.53	1.27	1.80
Cs	6.24	5.14	4.78	18.03	0.88	2.25	7.39	9.64
Ba	711.69	695.28	346.71	1439.27	117.30	194.73	890.01	1084.74
La	59.29	60.12	23.41	105.23	14.20	14.00	74.12	88.12
Ce	134.74	129.85	67.60	256.52	29.60	41.33	171.18	212.51
Eu	1.85	1.55	1.02	5.00	0.58	0.50	2.05	2.55
Gd	7.95	8.09	2.80	13.74	2.57	1.20	9.29	10.48
Tb	1.38	1.43	0.55	2.47	0.40	0.28	1.71	1.99
Dy	7.89	8.23	3.25	15.50	2.32	1.29	9.52	10.81
Ho	1.74	1.83	0.74	3.47	0.44	0.34	2.17	2.51
Er	5.35	5.61	2.39	10.90	1.21	1.00	6.62	7.62
Tm	1.15	1.02	0.69	2.43	0.16	0.63	1.66	2.29
Yb	5.60	5.78	2.75	10.37	1.00	1.45	7.23	8.67
Lu	1.22	1.11	0.75	2.66	0.14	0.72	1.84	2.56
Hf	6.39	4.49	6.61	22.30	0.04	2.95	7.45	10.40
Hg	0.04	0.03	0.04	0.15	0.01	0.01	0.03	0.04
Pb	53.63	39.00	40.65	181.10	11.93	16.39	55.39	71.78
Th	41.10	37.61	29.98	116.09	3.50	24.81	62.42	87.23
U	6.04	5.70	4.30	17.63	0.60	2.61	8.31	10.92
Bi	0.23	0.09	0.28	0.99	0.01	0.08	0.17	0.25
Nb	4.05	0.04	6.41	16.80	0.00	0.04	0.08	0.12
W	1.02	0.00	1.67	5.30	0.00			
Zr	145.31	0.95	252.51	797.20	0.00	0.95	1.90	2.85

To quantify the degree of elemental enrichment in rocks and soils, Pollution Index (PI) values were calculated using:

$$PI = \frac{C_{sample}}{C_{reference}}$$

where C_{sample} represents the measured concentration and $Cr_{eference}$ corresponds to the UCC value of Rudnick and Gao [92]. PI provides a straightforward measure of the relative enrichment or depletion of an element in comparison to natural crustal abundances. Based on commonly adopted classification schemes:

PI < 1 → Element is depleted or at sub-background levels

PI = 1 → Element concentration is consistent with natural background conditions
PI > 1 → Element shows enrichment relative to background values

In this study, PI > 1.5 was considered indicative of notable or significant enrichment, highlighting elements that depart markedly from typical crustal concentrations and may therefore reflect geochemical processes such as magmatic differentiation, hydrothermal alteration, or supergene mobility.

The Index of Geo-accumulation (*Igeo*), first introduced by Müller [93], is widely employed in geochemical and environmental assessments to evaluate the degree of elemental enrichment in soils, sediments, and rocks. Unlike simple enrichment ratios, the Igeo formulation considers not only potential contamination but also natural geochemical variability. This enables a more nuanced interpretation of elemental anomalies.

Igeo is defined as follows:

$$Igeo = Log_2 \frac{C_{sample}}{1.5xC_{reference}} = Log_2 \frac{PI}{1.5}$$

where C_{sample} is the measured concentration and $C_{reference}$ is typically the average composition of the upper continental crust (UCC).

The 1.5 correction factor is a critical component of the index and is included to:

- compensate for natural background fluctuations of approximately ±0.5-fold,
- reduce the influence of analytical uncertainties,
- account for local lithological or geochemical heterogeneity,
- enhance the robustness of comparisons across different regions and depositional environments.

By applying a logarithmic scale, Igeo offers several advantages:

- normalizes wide concentration ranges,
- provides meaningful sensitivity even at low element abundances,
- supports consistent comparisons among different elements, sampling sites, and lithologies,
- improves interpretability of subtle deviations from natural background levels.

Müller's classification categorizes the degree of enrichment or pollution into seven classes (Table 3):

Table 3. Müller's classification of degree of enrichment or pollution

Igeo Range	**Class**	**Enrichment / Pollution Status**
Igeo ≤ 0	0	Practically unpolluted
0 < Igeo ≤ 1	1	Unpolluted to slightly polluted
1 < Igeo ≤ 2	2	Moderately polluted
2 < Igeo ≤ 3	3	Moderately to strongly polluted
3 < Igeo ≤ 4	4	Strongly polluted
4 < Igeo ≤ 5	5	Strongly to extremely polluted
Igeo > 5	6	Extremely polluted

This classification provides a standardized interpretative framework that is widely used in environmental geochemistry, soil pollution studies, and exploration geochemistry to differentiate between natural geochemical anomalies and anthropogenic contributions.

When the major oxide composition of the investigated rock units is assessed using both the Pollution Index (PI) and the Geo-accumulation Index (*Igeo*), the elements generally exhibit PI values clustering around ~1.0. Such values indicate that the elemental abundances within the rocks are broadly consistent with average upper crustal concentrations and do not display notable deviations from the expected geochemical background. Likewise, the calculated *Igeo* values, which predominantly fall near −0.5, correspond to the "practically unpolluted" category as defined by Müller (1969). This classification implies that the detected concentrations can be attributed primarily to natural lithological variability rather than to any external enrichment or contamination. Overall, the PI and *Igeo* results suggest that the major oxides are geochemically stable and show no significant enrichment trends, supporting the interpretation that the compositions of the rocks largely reflect their intrinsic petrogenetic signatures rather than secondary modification or anthropogenic input.

When the trace-element composition of the studied rocks is evaluated using the relevant geochemical indices, distinct enrichment and depletion patterns become evident. Elements such as Co, Cs, V, Ni, and Pb yield PI values lower than 0.5 and *Igeo* values below −1.5 (Table 1, Figure 2), indicating that these elements are markedly depleted relative to average crustal abundances. This pronounced deficiency suggests that their concentrations are primarily controlled by the intrinsic mineralogical composition of the host rock rather than by secondary processes.

In contrast, elements including Ba, Ga, Y, and the rare earth elements (e.g., Sm, Eu, Gd) exhibit PI values exceeding 1.1 and *Igeo* values greater than −0.4 (Table 1 and Figure 2). These metrics point to slight enrichment within the rock matrix. Such enrichment is plausibly associated with the presence of secondary mineral phases—particularly barite and clay minerals—or may reflect the influence of hydrothermal alteration, which can preferentially mobilize and concentrate these elements.

Comparison of the mean, median, and geometric mean values of trace-element concentrations through dispersion plots (Figure 2) shows that these three statistical parameters display broadly comparable trends. This convergence implies that the dataset is not strongly skewed and that extreme outliers are minimal. Therefore, the arithmetic mean can be considered a suitable and representative local background value for the trace-element content of the investigated rock samples.

Descriptive statistics for the elemental concentrations of soils developed on the Gümüşhane Granitoid were determined to establish their geochemical characteristics (Table 4). Given the presence of several extreme values in the dataset, the median was adopted as the most representative measure of central tendency for soil geochemistry. For threshold calculations, Median + MAD and Median + 2×MAD values were employed to define conservative and elevated anomaly limits, respectively (Figure 3). This approach provides a robust means of identifying geochemical anomalies in datasets that deviate from normality.

Evaluation of Pollution Index (PI) values for the soils reveals pronounced enrichments relative to upper crustal abundances. Specifically, the elements P, Mn, As, Y, Cd, Sn, Sb, La, Ce, Sm, Eu, Gd, Tb, Dy, Ho, Er, Tm, Yb, Lu, Pb, Th, and U exhibit PI values exceeding 1.5 (Table 4; Figure 3). These enrichments suggest that the local soils systematically contain higher background levels of these elements compared to global crustal averages.

Consequently, prospection and exploration geochemical studies in the region should consider these elevated local thresholds rather than relying solely on upper-crust reference values. Incorporating locally calibrated threshold levels will enhance the accuracy of anomaly detection and reduce the likelihood of false positives or misinterpretation arising from naturally enriched soil geochemical signatures.

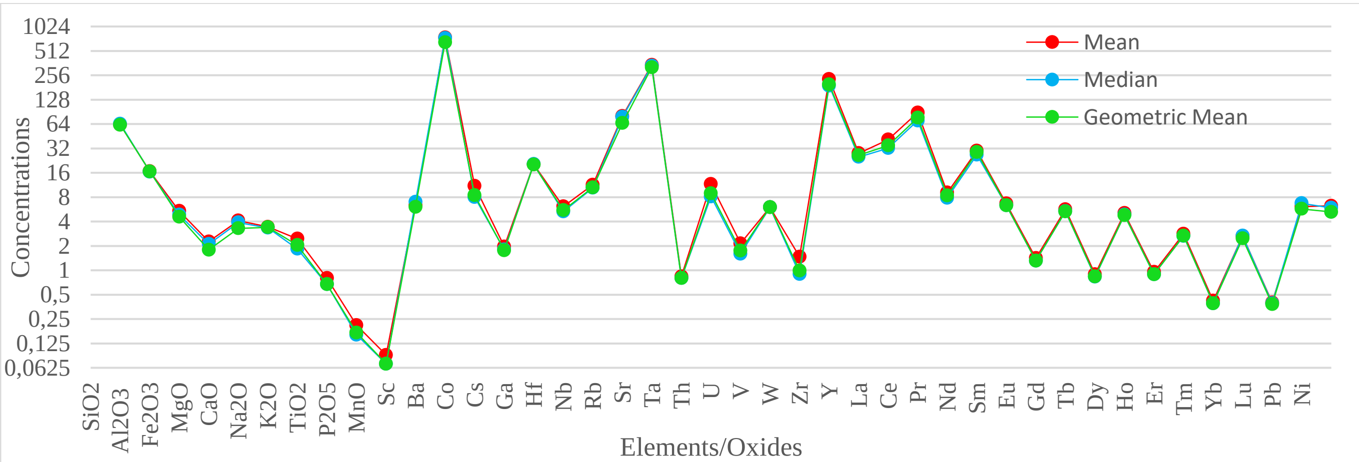

Figure 2. Scatter–curve diagram comparing the arithmetic mean, median, and geometric mean concentrations of major oxides and trace elements in the Gümüşhane Granitoid. *Major oxides are expressed in wt.%, whereas trace elements are given in ppm. The vertical axis is plotted on a base-2 logarithmic scale.*

Table 4. PI and Igeo indices of some elements in soils from the Çamlıköy and Işıkdere areas. Values with PI > 1.5 are highlighted in bold.

PI	PI (Mean)	PI (Median)	Igeo (Mean)
Mg	0.76	0.76	-0.98
P	**15.18**	**12.89**	3.34
K	1.04	0.87	-0.53
Ca	0.65	0.37	-1.21
Sc	1.35	1.43	-0.15
V	1.13	1.2	-0.41
C	0.49	0.42	-1.62
Mn	**1.89**	**1.8**	0.33
Fe	1.49	1.42	-0.01
Co	0.87	0.79	-0.79
Ni	0.37	0.33	-2.02
Cu	1.07	0.85	-0.49
Zn	2.27	1.41	0.60
As	**3.21**	**2.21**	1.10
Rb	1.45	1.48	-0.05
Sr	0.3	0.25	-2.32
Y	**2.01**	**2.23**	0.42
Mo	**1.87**	1.15	0.32
Cd	**7.16**	**3.17**	2.25
Sn	**3.09**	**3.1**	1.04
Sb	**3.12**	**1.84**	1.06
Cs	1.27	1.05	-0.24
Ba	1.14	1.11	-0.40
La	**1.91**	**1.94**	0.35
Ce	**2.14**	**2.06**	0.51
Pr	1.29	1.32	-0.22
Nd	0.97	1.07	-0.63
Sm	**1.83**	**1.87**	0.29
Eu	**1.85**	**1.55**	0.30
Gd	**1.99**	**2.02**	0.41
Tb	**1.98**	**2.04**	0.40
Dy	**2.02**	**2.11**	0.43
Ho	**2.1**	**2.2**	0.49
Er	**2.33**	**2.44**	0.64
Tm	**3.83**	**3.41**	1.35
Yb	**2.8**	**2.89**	0.90
Lu	**3.93**	**3.59**	1.39
Hf	1.2	0.85	-0.32
Hg	0.77	0.51	-0.96
Pb	**3.15**	**2.29**	1.07
Th	**3.91**	**3.58**	1.38
U	**2.24**	**2.11**	0.58
Bi	1.45	0.56	-0.05
Nb	0.34	0	-2.14
Ta	0.47	0	-1.67
W	0.54	0	-1.47
Zr	0.75	0	-1.00

An integrated evaluation of the PI and Igeo indices for the soils within the study area reveals that the analyzed elements cluster into four principal behavioral groups. These groups provide critical insight into both natural geochemical controls linked to parent rock–soil interactions and the extent of potential anthropogenic influence.

a) Critical Contaminants (*Igeo* > 1)

Elements such as P, Cd, Lu, Tm, Th, As, Sb, Pb, and Sn exhibit pronounced enrichment, with both PI and

Igeo values indicating substantial deviation from background geochemical conditions. P and Cd, which present exceptionally high enrichment levels (PI > 7; *Igeo* ≥ 2), are consistent with hydrothermal alteration and (possible) intensive agricultural fertilizer application.

The elevated *Igeo* values of Lu, Tm, and Th—classified within the moderate to strong contamination range—can be attributed to the intrinsic LREE–HREE characteristics of the granitoid source as well as the strong affinity of fine-grained soil constituents (clays, Fe–Mn oxides, amorphous phases) for REE retention. Similarly, As, Sb, Pb, and Sn, which fall into the moderately polluted class, likely reflect contributions from historical metallurgical activities, legacy mining, or hydrothermal signatures inherited from the underlying geology.

b) Moderately Enriched Elements (0 < *Igeo* ≤ 1)

This category is dominated by rare earth elements (REE)—including Yb, Er, Ce, Ho, Dy, Y, Gd, Tb, La, Eu, and Sm—whose coherent geochemical behavior suggests a shared source and comparable controls on mobility and retention. PI values between ~1.8 and 2.8 imply that, beyond the granitoid-derived natural REE inventory, adsorption onto clay minerals, Fe–Mn oxyhydroxides, and amorphous constituents contributes significantly to their enrichment. Elements such as Zn, Mn, Mo, and U also display mild enrichment. Their patterns likely reflect combined inputs from natural weathering processes and localized anthropogenic activities (e.g., agricultural amendments, minor metallurgical contributions). The elevated U values (PI > 2) further support both phosphate fertilizer inputs (?) and the natural U content of the granitoid unit.

c) Elements Near Natural Background Levels (–1 < *Igeo* ≤ 0)

Elements in this group—such as Fe, Rb, Bi, Sc, Cs, Ba, V, Cu, Nd, and Hf—show minimal deviation from crustal norms and appear only weakly affected by external inputs. Their PI values, typically close to unity, reflect a strong geochemical continuity between the soils and the granitoid parent material. Sc and Cs, often regarded as conservative or reference elements in geochemical surveys, display limited variability, reinforcing the interpretation that the soil signatures remain largely governed by natural lithological controls.

d) Strongly Depleted Elements (*Igeo* ≤ –1)

Elements including Sr, Ni, Nb, C, Ta, W, Zr, Mg, Hg, Ca, and Co exhibit notable depletion compared with upper-crustal benchmarks. The depletion of Sr and Ca is consistent with enhanced leaching during prolonged chemical weathering, due to the high mobility of carbonate-bound phases. Low PI values for Ni, Co, and Mg support the absence of significant ultramafic or mafic rock contributions in the region. The systematic depletion of HFSE elements such as Nb, Ta, and Zr likely reflects the mineralogical characteristics of the granitoid, particularly the low abundance of zircon and related accessory phases. The low Hg concentrations indicate that the natural Hg background level in the area is inherently low.

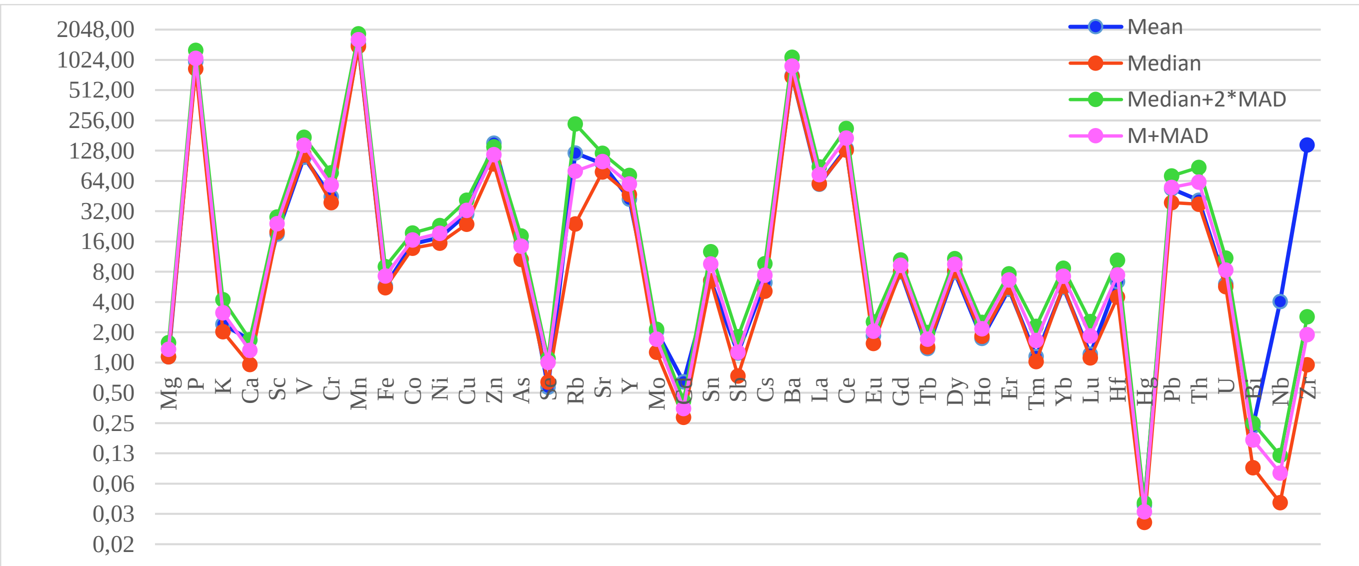

Figure 2. Line–scatter diagram showing the median, Median+MAD, and Median+2×MAD values of element concentrations in soils from the Çamlıköyü and Işıkdere areas

Combined interpretation of the PI–*Igeo* dataset demonstrates that anthropogenic and dominantly hydrothermal influences are most pronounced for elements such as P, Cd, As, Sb, Pb, and Sn. In contrast, many other elements retain signatures aligned with natural geochemical baselines. The coherent behavior of REEs highlights the prominent role of both the granitoid's primary REE composition and the sorptive capacity of fine-grained soil phases. In contrast, the depleted elements are primarily controlled by mineralogical constraints and weathering dynamics.

These findings underscore that local background concentrations and threshold values may diverge substantially from global upper-crustal averages, emphasizing the necessity of establishing site-specific geochemical baselines for reliable mineral exploration and environmental assessments.

4. Conclusions

This study successfully established site-specific geochemical baseline and threshold values for the Gümüşhane Granitoid and its derived soils in the Çamlıköy and Işıkdere districts, utilizing a robust statistical framework incorporating descriptive statistics, the Pollution Index (PI), and the Index of Geoaccumulation (*Igeo*). The research addresses the critical need for locally calibrated reference values in a major metallogenic belt, bridging the gap between exploration and environmental geochemistry objectives.

The key conclusions are summarized as follows:

- Rock Geochemistry Reflects Petrogenesis: The major oxide composition of the Gümüşhane Granitoid is broadly consistent with Upper Continental Crust (UCC) values (PI ~1.0; Igeo ~-0.5), reflecting its intrinsic, largely stable petrogenetic signature. Trace element analysis reveals distinct depletion of mafic elements (Co, Ni, V) and Pb, consistent with the felsic nature of the granitoid.
- Soil Geochemistry Demonstrates Substantial Local Enrichment: Soil concentrations of numerous elements (P, Mn, As, Cd, Sn, Sb, Pb, Th, U, and REEs) exhibit pronounced enrichment, with PI values significantly exceeding 1.5 relative to global UCC standards. This highlights the systemic divergence of the local geochemical background.
- Identification of Dual Enrichment Sources:
    - Anthropogenic/Hydrothermal Risk: Elements classified as Critical Contaminants (Igeo > 1), notably P, Cd, As, Sb, and Pb, strongly indicate inputs from external sources. The exceptional enrichment of P and Cd is plausibly linked to intensive agricultural practices (fertilizer input), while As, Sb, and Pb reflect potential contributions from historical mining/metallurgical activities or strong underlying hydrothermal signatures.
    - Natural Pedogenic and Lithological Controls: The coherent enrichment of Rare Earth Elements (REEs) (Yb, Er, Ce, etc.) is primarily controlled by the REE-rich nature of the granitoid and the high retention capacity of secondary soil phases (clays, Fe-Mn oxides) during weathering. The strong depletion of mobile elements (Sr, Ca) and HFSEs (Nb, Zr, \ Ta) further confirms that chemical weathering and the parent rock's mineralogical composition dictate the behavior of these elements.
- Methodological Strength for Anomaly Detection: The use of Median + MAD and Median + 2xMAD estimators provided robust, non-parametric local threshold values, effectively minimizing the influence of extreme outliers (Figure 2).

In conclusion, this research confirms that using global Upper Crustal values as a reference in the Gümüşhane region would lead to an unacceptable rate of false-positive anomalies in mineral exploration. The established local geochemical thresholds are therefore indispensable for reliable mineral prospection and for accurately defining the true extent of environmental contamination by differentiating between naturally elevated background levels and human-induced pollution. This study provides a vital scientific benchmark for future land-use planning and resource management in this important Turkish metallogenic province.

Acknowledgement

This study incorporates partial use of the data generated within the scope of the TÜBİTAK-funded Project No. 115Y146, and the authors gratefully acknowledge TÜBİTAK for the support provided. The author would like to express sincere gratitude to the Editor and the anonymous reviewers for their insightful comments and constructive suggestions during the peer-review process. Their expertise and feedback have significantly contributed to improving the quality and clarity of this manuscript.

References

[1]. Vural A, Kaygusuz A. The Geostatistical Evaluation of the Genetic Relationship of Rocks : A Case Study of the Derinoba-Kayadibi Granites. J Eng Res Appl Sci 2024; 13:2537–2552.

[2]. Vural A, Erşen F. Geology, mineralogy and geochemistry of manganese mineralization in Gumushane, Turkey. J Eng Res Appl Sci 2019; 8:1051–1059.

[3]. Vural A, Gündoğdu A, Saka F, Bulut VN. Geochemical investigation of the potability of surface water in Çit Stream and related creeks in Avliyana Basin (Gümüşhane , NE Türkiye). Turkish J Anal Chem 2022; 4:44–51.

[4]. Vural A. On the elemental contents of aspen (Populus tremula L.) leaves grown in the mineralization area. J Geogr Cartogr 2023; 6:1–10.

[5]. Vural A. Avliyana Cevherleşme/Alterasyon Sahasının Kütle Değişim Özellikleri ve Asit Maden Drenaj Potansiyelinin Araştırılması. Icontech Int J Surv Eng Technol 2022; 6:1–23.

[6]. Vural A. Evaluation of soil geochemistry data of Canca Area (Gümüşhane, Turkey) by means of Inverse Distance Weighting (IDW) and Kriging methods-preliminary findings. Bull Miner Res Explor 2019; 158:195–216.

[7]. Vural A, Kaya S, Başaran N, Songören OT. Anadolu Madenciliğinde İlk Adımlar. Ankara, Türkiye: Maden Tetkik ve Arama Genel Müdürlüğü, MTA Kültür Serisi-3; 2009.

[8]. Vural A, Safari S. Phytoremediation ability of Helichrysum arenarium plant for Au and Ag: case study at Demirören village (Gümüşhane, Turkey). Gold Bull 2022; 55:129–136.

[9]. Vural A, Akpinar İ, Sipahi F. Mineralogical and Chemical Characteristics of Clay Areas, Gümüşhane Region (NE Turkey), and Their Detection Using the Crósta Technique with Landsat 7 and 8 Images. Nat Resour Res 2021; 30:3955–3985.

[10]. Vural A, Çicek B. Evaluation of Gümüştuğ Antimonite (Torul , Gümüşhane/Türkiye) Mineralization with Soil Geochemistry and Multivariate Geostatistical Studies. J Eng Res Appl Sci 2022; 11:2156–2170.

[11]. Vural A. Demirören/Gümüşhane-Türkiye Kuvars Porfiri Kayacı ve İlişkili Skarn-Metasomatizmanın Jeokimyasal Özellikleri. Euroasia J Math Eng Nat Med Sci 2020; 7:97–121.

[12]. Özkan M, Vural A, Akgül Ö, Gültepe MA, Bayraktar C, Kara RT. Comprehensive geostatistical Assessment of stream sediments for mineralization potential in the eastern Black Sea region. Period Di Mineral 2025; 94:83–111.

[13]. Vural A, Kaya A. Arzular-Yitirmez-Dölek (Gümüşhane) Maden/Alterasyon Sahalarındaki Doğal (226Ra, 232Th ve 40K) ve yapay (138Cs) Radyoaktivitelerine ait ilk değerlendirmeler. Euroasia J Math Eng Nat Med Sci 2021; 8:105–120.

[14]. Vural A. Trace element accumulation behavior, ability, and propensity of Taraxacum officinale F.H. Wigg (Dandelion). Environ Sci Pollut Res 2024; 31:16667–16684.

[15]. Vural A, Kaya A. Assessment of Karamustafa Gold-Bearing Zn-Pb Mine (Gümüşhane, Türkiye) Area in Terms of Natural and Artificial Radioactivity. Göbeklitepe Int J Med Sci 2023; 6:39–52.

[16]. Vural A. Trace/heavy metal accumulation in soil and in the shoots of acacia tree, Gümüşhane-Turkey. Bull Miner Res Explor 2014; 148:85–106.

[17]. Hou Z, Zhang H. Geodynamics and metallogeny of the eastern Tethyan metallogenic domain. Ore Geol Rev 2015; 70:346–384.

[18]. Ünal Çakır E, Gökce A. Geology, fluid inclusion, and stable isotope (O, H, S, C) characteristics of the Hazinemağara (Gümüşhane) lead-zinc deposit , NE Turkey. Turkish J Earth Sci 2019; 28:623–639.

[19]. Akçay M, Lermi A, Van A. Biogeochemical exploration for massive sulphide deposits in areas of dense vegetation: An orientation survey around the Kankoy Deposit. J Geochemical Explor 1998; 63:173–187.

[20]. Lermi A. Midi (Karamustafa/Gümüşhane, KD Türkiye) Zn-Pb Yatağının Jeolojik, Mineralojik, Jeokimyasal ve Kökensel İncelemesi. Karadeniz Teknik Üniversitesi, Trabzon, 2003.

[21]. Vural A. Gold and Silver Content of Plant Helichrysum Arenarium, Popularly Known as the Golden Flower, Growing in Gümüşhane, NE Turkey. Acta Phys Pol A 2017; 132:978–980.

[22]. Vural A. Assessment of Sessile Oak (Quercus petraea L.) Leaf as Bioindicator for Exploration Geochemistry. Acta Phys Pol A 2016; 130:191–193.

[23]. Vural A, Çorumluoğlu Ö, Asri İ. Investigation of alteration areas by Crosta using LANDSAT images for Old Gumushane (Suleymaniye) and its near vicinity. J Nat Sci Inst Gumushane Univ 2012; 2:36–48.

[24]. Vural A, Corumluoglu Ö, Asri İ. Remote sensing technique for capturing and exploration of mineral deposit sites in Gumushane metallogenic province, NE Turkey. J Geol Soc India 2017; 90:628–633.

[25]. Vural A. Relationship between the geological environment and element accumulation capacity of Helichrysum arenarium. Arab J Geosci 2018; 11:258.

[26]. Reimann C, Garrett RG. Geochemical background - Concept and reality. Sci Total Environ 2005; 350:12–27.

[27]. Ellsmore R, Buckman S. Soil geochemistry and

pathfinder element distribution associated with the Hillgrove Antimony-Gold-Tungsten deposit, New England Orogen, NSW. New Engl Orogen 2010 2010; 2010:141–144.
[28]. Hao L, Zhao X, Zhao Y, Lu J, Sun L. Determination of the geochemical background and anomalies in areas with variable lithologies. J Geochemical Explor 2014; 139:177–182.
[29]. Vural A, Aydal D. Soil geochemistry study of the listvenite area of Ayvacik (Çanakkale, Turkey). Casp J Environ Sci 2020; 18:205–215.
[30]. Vural A. Biogeochemical characteristics of Rosa canina grown in hydrothermally contaminated soils of the Gümüşhane Province, Northeast Turkey. Environ Monit Assess 2015; 187:486.
[31]. Vural A. Soil geochemistry survey for gold exploration at Kısacık area (Çanakkale, Ayvacık, Türkiye). Period Di Mineral 2024; 93:61–83.
[32]. Zuo R, Wang J, Chen G, Yang M. Reprint of 'Identification of weak anomalies: A multifractal perspective'. J Geochemical Explor 2015; 154:200–212.
[33]. Matheron G. Principles of geostatistics. Econ Geol 1963; 58:1246–1266.
[34]. Hawkes HE, Webb JS. Geochemistry in Mineral Exploration. New York: Harper and Row; 1962.
[35]. Afzal P, Mirzaei M, Yousefi M, Adib A, Khalajmasoumi M, Zarifi AZ, Foster P, Yasrebi AB. Delineation of geochemical anomalies based on stream sediment data utilizing fractal modeling and staged factor analysis. J African Earth Sci 2016; 119:139–149.
[36]. Templ M, Filzmoser P, Reimann C. Cluster analysis applied to regional geochemical data: Problems and possibilities. Appl Geochemistry 2008; 23:2198–2213.
[37]. Daya AA. Comparative study of C-A, C-P, and N-S fractal methods for separating geochemical anomalies from background: A case study of Kamoshgaran region, northwest of Iran. J Geochemical Explor 2015; 150:52–63.
[38]. Topuz G, Altherr R, Kalt A, Satir M, Werner O, Schwarz WH. Aluminous granulites from the Pulur complex, NE Turkey: A case of partial melting, efficient melt extraction and crystallisation. Lithos 2004; 72:183–207.
[39]. Kaygusuz A, Arslan M, Siebel W, Sipahi F, Ilbeyli N. Geochronological evidence and tectonic significance of Carboniferous magmatism in the southwest Trabzon area, eastern Pontides, Turkey. Int Geol Rev 2012; 54:1776–1800.
[40]. Kaygusuz A, Arslan M, Sipahi F, Temizel İ. U-Pb zircon chronology and petrogenesis of Carboniferous plutons in the northern part of the Eastern Pontides, NE Turkey: Constraints for Paleozoic magmatism and geodynamic evolution. Gondwana Res 2016; 39:327–346.
[41]. Kaygusuz A, Aydınçakır E, Yücel C, Atay HE. Petrographic and geochemical characteristics of carboniferous plutonic rocks around Erenkaya (Gümüşhane, NE Turkey). J Eng Res Appl Sci 2021; 10:1774–1788.
[42]. Kaygusuz A. Geochronological age relationships of Carboniferous Plutons in the Eastern Pontides (NE Turkey). J Eng Res Appl Sci 2020; 9:1299–1307.
[43]. Kaygusuz A, Yücel C, Aydınçakır E, Gücer MA, Ruffet G. 40Ar–39Ar dating, whole-rock and Sr-Nd isotope geochemistry of the Middle Eocene calc-alkaline volcanic rocks in the Bayburt area, Eastern Pontides (NE Turkey): Implications for magma evolution in an extension-related setting. Mineral Petrol 2022; 116:379–399.
[44]. Topuz G, Altherr R, Siebel W, Schwarz WH, Zack T, Hasözbek A, Barth M, Satir M, Şen C. Carboniferous high-potassium I-type granitoid magmatism in the Eastern Pontides: The Gümüşhane pluton (NE Turkey). Lithos 2010; 116:92–110.
[45]. Vural A, Kaygusuz A. Petrology of the Paleozoic Plutons in Eastern Pontides: Artabel Pluton (Gümüşhane, NE Turkey). J Eng Res Appl Sci 2019; 8:1216–1228.
[46]. Kaygusuz A. Petrographic and Geochemical characteristics of Paleozoic Gabbroic rocks around Taşdelen (Özdil / Trabzon, NE Türkiye). J Eng Res Appl Sci 2022; 11:2111–2122.
[47]. Ustaömer T, Robertson AHF, Ustaömer PA, Gerdes A, Peytcheva I. Constraints on variscan and cimmerian magmatism and metamorphism in the pontides (Yusufeli-Artvin area), NE Turkey from U-Pb dating and granite geochemistry. Geol Soc Spec Publ 2013; 372:49–74.
[48]. Saydam Eker C, Sipahi F, Kaygusuz A. Trace and Rare Earth Elements as Indicators of Provenance and Depositional Environments of Lias Cherts in Gumushane, NE, Turkey,. Chemie Der Erde - Geochemistry 2012; 72:167–177.
[49]. Ağar Ü. Demirözü (Bayburt) ve Köse (Kelkit) bölgesinin jeolojisi. İstanbul Üniversitesi, 1977.
[50]. Dokuz A, Karslı O, Chen B, Uysal I. Sources and petrogenesis of Jurassic granitoids in the Yusufeli area, Northeastern Turkey: Implications for pre- and post-collisional lithospheric thinning of the eastern Pontides. Tectonophysics 2010; 480:259–279.
[51]. Eyuboğlu Y, Dudas FO, Santosh M, Zhu DC, Yi K, Chatterjee N, Akaryalı E, Liu Z. Cenozoic forearc gabbros from the northern zone of the Eastern Pontides Orogenic Belt, NE Turkey: implications for slab window magmatism and convergent margin tectonics. Gondwana Res 2016; 33:160–190.
[52]. Karslı O, A D, Kandemir R. Zircon Lu-Hf

isotope systematics and U-Pb geochronology, whole-rock Sr-Nd isotopes and geochemistry of the early Jurassicssic Gokçedere pluton, Sakarya Zone-NE Turkey: a magmatic response to roll-back of the Paleo-Tethyan oceanic lithosphere. Contrib to Mineral Petrol 2017; 172:1–31.
[53]. Aydınçakır E, Yücel C, Kaygusuz A, Bilici Ö, Yi K, Jeong YJ, Güloğlu ZS. Magmatic evolution of the Calc-alkaline Middle Jurassic igneous rocks in the eastern pontides, NE Turkey: insights from geochemistry, whole-rock Sr-Nd-Pb, in situ zircon Lu-Hf isotopes, and U-Pb geochronology. Int Geol Rev 2023; 00:1–22.
[54]. Aydınçakır E, Gündüz R, Yücel C. Emplacement conditions of magma(s) forming Jurassic plutonic rocks in Gümüşhane (Eastern Pontides, Turkey). Bull Miner Res Explor 2020; 162:175–196.
[55]. Kaygusuz A, Arsan M, Sipahi F, Temizel İ, Yücel C, Çakmak G. Doğu Pontid Güney Zonu'ndaki (Bayburt) Tersiyer yaşlı intruzif kayaçların Petrokimyası, Jeokronolojisi ve İzotop Sistematikleri. Tübitak Projesi Sonuç Raporu, Proje No 115Y154, 2019:1–254.
[56]. Vural A, Kaygusuz A. Petrographic and geochemical characteristics of late Cretaceous volcanic rocks in the vicinity of Avliyana (Gümüşhane, NE Turkey). J Eng Res Appl Sci 2021; 10:1796–1810.
[57]. Köprübaşı N, Şen C, Kaygusuz A. Doğu Pontid adayayı granitoyidlerinin karşılaştırılmalı petrografik ve kimyasal özellikleri, KD Türkiye. Uygulamalı Yerbilim Derg 2000; 1:111–120.
[58]. Kaygusuz A, Arslan M, Temizel İ, Yücel C, Aydınçakır E. U–Pb zircon ages and petrogenesis of the Late Cretaceous I-type granitoids in arc setting, Eastern Pontides, NE Turkey. J African Earth Sci 2021; 174:104040.
[59]. Saydam Eker C, Korkmaz S. Mineralogy and whole rock geochemistry of late Cretaceous sandstones from the eastern Pontides (NE Turkey). Neues Jahrb Fur Mineral Abhandlungen 2011; 188:235–256.
[60]. Vural A, Akpınar İ, Kaygusuz A. Petrological characteristics of Cretaceous volcanic rocks of Demirören (Gümüşhane, NE Turkey) region. J Eng Res Appl Sci 2021; 10:1828–1842.
[61]. Topuz G, Altherr R, Schwarz WH, Siebel W, Satır M, Dokuz A. Post-collisional plutonism with adakite-like signatures: The Eocene Saraycik granodiorite (Eastern Pontides, Turkey). Contrib to Mineral Petrol 2005; 150:441–455.
[62]. Karslı O, Ketenci M, Uysal I, Dokuz A, Aydin F, Chen B, Kandemir R, Wijbrans J. Adakite-like granitoid porphyries in the Eastern Pontides, NE Turkey: Potential parental melts and geodynamic implications. Lithos 2011; 127:354–372.
[63]. Dokuz A, Uysal I, Siebel W, Turan M, Duncan R, Akçay M. Post-collisional adakitic volcanism in the eastern part of the Sakarya Zone, Turkey: Evidence for slab and crustal melting. Contrib to Mineral Petrol 2013; 166:1443–1468.
[64]. Temizel İ, Arslan M, Yücel C, Abdioğlu Yazar E, Kaygusuz A, Aslan Z. Eocene tonalite–granodiorite from the Havza (Samsun) area, northern Turkey: adakite-like melts of lithospheric mantle and crust generated in a post-collisional setting. Int Geol Rev 2020.
[65]. Arslan M, Temizel İ, Abdioğlu E, Kolaylı H, Yücel C, Boztuğ D, Şen C. 40Ar–39Ar dating, whole-rock and Sr–Nd–Pb isotope geochemistry of post-collisional Eocene volcanic rocks in the southern part of the Eastern Pontides (NE Turkey): implications for magma evolution in extension-induced origin. Contrib to Mineral Petrol 2013; 166:113–142.
[66]. Kaygusuz A, Arslan A, Siebel W, Şen C. Geochemical and Sr-Nd Isotopic Characteristics of Post-Collisional Calc-Alkaline Volcanics in the Eastern Pontides (NE Turkey). Turkish J Earth Sci 2011; 20:137–159.
[67]. Aslan Z, Arslan M, Temizel İ, Kaygusuz A. K-Ar dating, whole-rock and Sr-Nd isotope geochemistry of calc-alkaline volcanic rocks around the Gümüşhane area: Implications for post-collisional volcanism in the Eastern Pontides, Northeast Turkey. Mineral Petrol 2014; 108:245–267.
[68]. Temizel İ, Arslan M, Ruffet G, Peucat JJ. Petrochemistry, geochronology and Sr–Nd isotopic systematics of the Tertiary collisional and post-collisional volcanic rocks from the Ulubey (Ordu) area, eastern Pontide, NE Turkey: Implications for extension-related origin and mantle source characteristi. Lithos 2012; 128–131:126–147.
[69]. Kaygusuz A, Merdan Tutar Z, Yücel C. Mineral chemistry, crystallization conditions and petrography of Cenozoic volcanic rocks in the Bahçecik (Torul/Gumushane) area, Eastern Pontides (NE Turkey). J Eng Res Appl Sci 2017; 6:641–651.
[70]. Kaygusuz A, Gucer MA, Yücel C, Aydınçakır E, Sipahi F. Petrography and crystallization conditions of Middle Eocene volcanic rocks in the Aydıntepe-Yazyurdu (Bayburt) area, Eastern Pontides (NE Turkey). J Eng Res Appl Sci 2019; 8:1205–1215.
[71]. Yücel C, Arslan M, Temizel İ, Abdioğlu Yazar E, Ruffet G. Evolution of K-rich magmas derived from a net veined lithospheric mantle in an ongoing extensional setting: Geochronology and geochemistry of Eocene and Miocene volcanic rocks from Eastern Pontides (Turkey). Gondwana Res 2017; 45:65–86.
[72]. Kaygusuz A, Sahin K. Petrographical , geochemical and petrological characteristics of

Eocene volcanic rocks in the Mescitli area , Eastern Pontides (NE Turkey). J Eng Res Appl Sci 2016; 5:473–486.
[73]. Vural A, Akpınar İ, Kaygusuz A, Sipahi F. Petrological characteristics of Eocene volcanic rocks around Demirören (Gümüşhane, NE Turkey). J Eng Res Appl Sci 2021; 10:1703–1716.
[74]. Vural A, Kaygusuz A. Geochronology, petrogenesis and tectonic importance of Eocene I-type magmatism in the Eastern Pontides, NE Turkey. Arab J Geosci 2021; 14:467.
[75]. K Vural A. K-Ar dating for determining the age of mineralization as alteration product: A case study of antimony mineralization vein type in granitic rocks of Gümüşhane area, Turkey. Acta Phys Pol A 2017; 132:792–795.
[76]. Kaygusuz A, Öztürk M. Geochronology, geochemistry, and petrogenesis of the Eocene Bayburt intrusions, Eastern Pontide, NE Turkey: implications for lithospheric mantle and lower crustal sources in the high-K calc-alkaline magmatism. J Asian Earth Sci 2015; 108:97–116.
[77]. Özdamar Ş, Roden MF, Billor MZ. Petrology of the shoshonitic Çambaşı pluton in NE Turkey and implications for the closure of the Neo-Tethys Ocean: insights from geochemistry, geochronology and SrNd isotopes. Lithos 2017; 284–285:477–492.
[78]. Eyüboğlu Y, Dudas FO, Thorkelson D, Zhu DC, Liu Z, Chatterjee N, Yi K, Santosh M. Eocene granitoids of northern Turkey: Polybaric magmatism in an evolving arc–slab window system. Gondwana Res 2017; 50:311–345.
[79]. Kaygusuz A, Yücel C, Arslan M, Sipahi F, Temizel İ, Çakmak G, Güloğlu ZS. Petrography, mineral chemistry and crystallization conditions of Cenozoic plutonic rocks located to the north of Bayburt (Eastern Pontides, Turkey). Bull Miner Res Explor 2018; 157:75–102.
[80]. Kaygusuz A, Yücel C, Arslan M, Temizel İ, Yi K, Jeong Y-J, Siebel W, Sipahi F. Eocene I-type magmatism in the Eastern Pontides, NE Turkey: Insights into magma genesis and magma-tectonic evolution from whole-rock geochemistry, geochronology and isotope systematics. Int Geol Rev 2020.
[81]. Temizel İ, Abdioğlu Yazar E, Arslan M, Kaygusuz A, Aslan Z. Mineral chemistry, whole-rock geochemistry and petrology of Eocene I-type shoshonitic plutons in the Gölköy area (Ordu, NE Turkey). Bull Miner Res Explor 2018; 157:121–152.
[82]. Aydın F, Karslı O, Chen B. Petrogenesis of the Neogene alkaline volcanics with implications for post-collisional lithospheric thinning of the Eastern Pontides, NE Turkey. Lithos 2008; 104:249–266.
[83]. Karslı O, Dokuz A, Aydın F, Uysal İ, Şengün F, Kandemir R, Santos JF, Andersen T. Tracking the timing of Neotethyan oceanic slab break-off: Geochronology and geochemistry of the quartz diorite porphyries, NE Turkey. J Asian Earth Sci 2020; 200.
[84]. Yücel C, Arslan M, Temizel İ, Abdioğlu E. Volcanic facies and mineral chemistry of Tertiary volcanics in the northern part of the Eastern Pontides, northeast Turkey: implications for pre-eruptive crystallization conditions and magma chamber processes. Mineral Petrol 2014; 108:439–467.
[85]. Vural A, Külekçi G. Zenginleştirilmiş Jeoturizm Güzergahı:Gümüşhane-Bahçecik Köyü. Euroasia J Math Eng Nat Med Sci 2021; 8:1–23.
[86]. Vural A. Zenginleştirilmiş Jeoturizm Güzergahlarına Dair Farkındalık Oluşturulması : Eski Gümüşhane - Dörtkonak Güzergahı. Gümüşhane Üniversitesi Sos Bilim Enstitüsü Elektron Derg 2019; 10:250–274.
[87]. Vural A, Gundogdu A, Akpinar I, Baltaci C. Environmental impact of Gümüşhane City, Turkey, waste area in terms of heavy metal pollution. Nat Hazards 2017; 88:867–890.
[88]. Vural A, Şahin E. Gümüşhane Şehir Merkezinden Geçen Karayolunda Ağır Metal Kirliliğine Ait İlk Bulgular. Gümüşhane Üniversitesi, Fen Bilim Enstitüsü Derg 2012; 2:21–35.
[89]. Bulut VN, Gundogdu A, Duran C, Senturk HB, Soylak M, Elci L, Tufekci M. A multi-element solid-phase extraction method for trace metals determination in environmental samples on Amberlite XAD-2000. J Hazard Mater 2007; 146:155–163.
[90]. Dokuz A. A slab detachment and delamination model for the generation of Carboniferous high-potassium I-type magmatism in the Eastern Pontides, NE Turkey: The Köse composite pluton. Gondwana Res 2011; 19:926–944.
[91]. Vural A, Gündoğdu A, Bulut VN, Alemdağ S, Saka F, Soylak M. Harşit Vadisinde (Gümüşhane), Bölgedeki (Terkedilmiş) Maden Sahalarından Kaynaklanan Ağır Metal/İz Element Kirliliğinin Araştırılması. Gümüşhane, Türkiye: 2020.
[92]. Rudnick R, Gao S. Composition of the Continental Crust. In: Holland H, Turekian K (eds.), Readings of Treatise on Geochemistry. 2nd ed. Londan, England: Elsevier; 2010:101–123.
[93]. Muller G. Index of geoaccumulation in sediments of the Rhine River. Geol J 1969; 2:108–118.